

# Static Magnetic Properties and Morphological Behaviour of Mn And Zn Substituted Ca-Hexaferrite by Ceramic Technic

Chandrakant L. Khobaragade

Department of Applied Physics, GovindraoWanjari College of Engineering & Tech., Nagpur, India.

## ABSTRACT:

Synthesis of M-type hexagonal ferrite compounds,  $\text{Ca}(\text{CoTi})_{0.5}(\text{MnZn})_{x/2}\text{Fe}_{11-x}\text{O}_{19}$  ( $x = 0.0, 0.2, 0.4, 0.6, 0.8, 1.0, 1.2$ ) prepared by ceramic technic. Mn and Zn ions substituted to find the magnetic characterization at magnetic field of 10 kOe. XRD and SEM study have been done for getting the hexagonal structure of these samples. Due to the substitution of Mn and Zn ions saturation magnetization increases and magnetocrystalline anisotropy decreases. Due to the sub-lattice site distribution the variations in magnetic parameters have been observed. Because of Mn and Zn ions substitution Curie temperature decreases by weakening of superexchange interaction. These materials can be used for various applications such as permanent magnetic material, magnetic recording media, ferrofluids, sensors, microwave absorbing materials, ceramic magnets in loud speakers and rotors in small DC motors by studying various magnetic parameters from VSM characterization.

**Keywords:** XRD, SEM, Magnetic properties, Hexaferrite.

## 1. INTRODUCTION:

Ferroxdure  $\text{MFe}_{12}\text{O}_{19}$  hexagonal ferrites, specifically calcium hexaferrites, are renowned for their uniaxial magneto-crystalline anisotropy, emphasizing increased magnetization along the c-axis [1, 2]. Widely used in magnetic recording media due to their intrinsic properties, these hexagonal ferrites exhibit tunable magnetic characteristics like coercivity and saturation magnetization through the substitution of  $\text{Fe}^{3+}$  ions in the crystal sublattice [3, 4]. The electronic configuration and site distribution of substituting cations play a crucial role in determining these properties. Notably, the substitution of ions with intrinsic coercivity effectively decreases, while saturation magnetization increases, making them valuable for magnetic recording applications [5]. Ongoing efforts focus on reducing coercive force while simultaneously enhancing magnetization through substitution. The application of hexagonal ferrites in magnetic recording media necessitates precise control over homogeneity and morphology. In this context, detailed research on substituted Ca-hexaferrite, specifically with Mn and Zn ions, has been undertaken using the ceramic method. While An et al. employed the sol-gel method for magnetic property investigation [6], Parkin et al. synthesized similar ferrites through the self-propagating high-temperature method [7]. The current study delves into the magnetic properties of Mn and Zn ions substituted CaM ferrite, contributing to the ongoing exploration of advanced materials in this domain.

## 2. EXPERIMENTAL:

Polycrystalline M-type hexagonal ferrites  $\text{Ca}(\text{CoTi})_{0.5}(\text{MnZn})_{x/2}\text{Fe}_{11-x}\text{O}_{19}$ ,  $x = 0.0-1.2$ ) were synthesized via standard ceramic technique or solid-state diffusion. High-purity analytical reagents ( $\text{CaO}$ ,  $\text{CoO}$ ,  $\text{ZnO}$ ,  $\text{MnO}_2$ ,  $\text{TiO}_2$ , and  $\text{Fe}_2\text{O}_3$ ) were used for sample preparation, with oxides mixed in stoichiometric ratios. Initially, the compounds' powders were crushed in an agate pestle mortar for 6 hours, pre-sintered at  $500^\circ\text{C}$  for 10 hours, and finely ground again. Pellets were formed using polyvinyl acetate as a binder and hydraulic press. The compounds were synthesized at  $1040^\circ\text{C}$  for 96 hours, with slow heating and cooling at  $2^\circ\text{C}/\text{min}$ . Magnetic parameters were measured at 10kOe using a vibrating sample magnetometer. Curie temperature (TC) was determined using Gouy's balance method. X-ray diffraction and SEM were employed to study phase transitions and microstructure. The magnetic parameters were analyzed from room temperature to  $700^\circ\text{C}$ , revealing the material's transition from a ferrimagnetic to a paramagnetic state as the temperature increased.

## 3. RESULTS AND DISCUSSION:

### 3.1. XRD

X-ray diffraction (Fig.1) studies and calculated data from the XRD it reveal that the studied materials are magnetoplumbite structure with relative intensity peaks indicating variations in lattice sites due to substituted ions. Structural data (Fig. 2) show minimal variation in lattice parameter 'a,' while 'c' initially decreases rapidly with substitution, consistent with M-type hexagonal standards [8]. The substitution of  $\text{Mn}^{4+}$  and  $\text{Zn}^{2+}$  ions leads to larger magnetization along the 'c'-axis than the 'a'-axis, attributed to the larger ionic radii of  $\text{Mn}^{4+}$  ( $0.60\text{\AA}$ ) and  $\text{Zn}^{2+}$  ions ( $0.74\text{\AA}$ ) compared to  $\text{Fe}^{3+}$  ions ( $0.64\text{\AA}$ ) [9, 10]. These changes in lattice constants and magnetic properties result from superexchange interactions with the substituted ions.

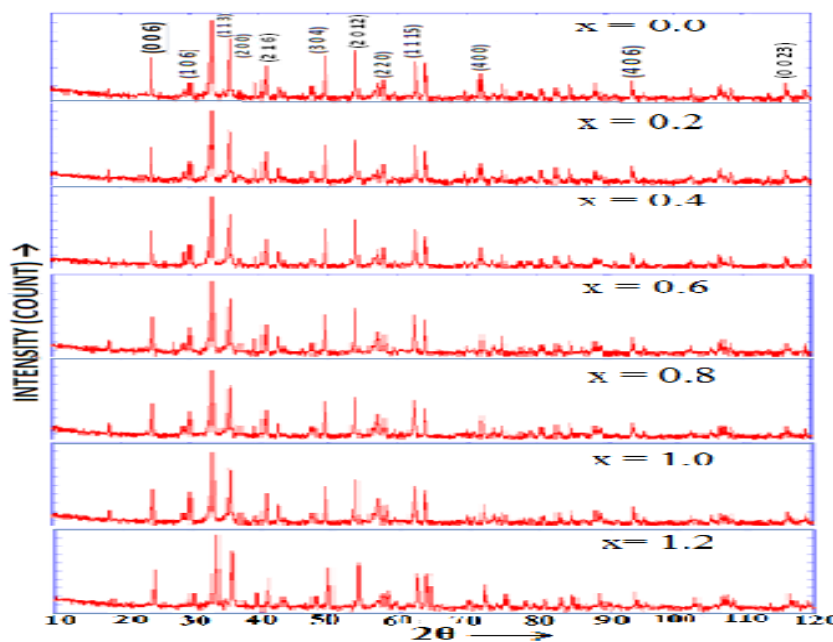
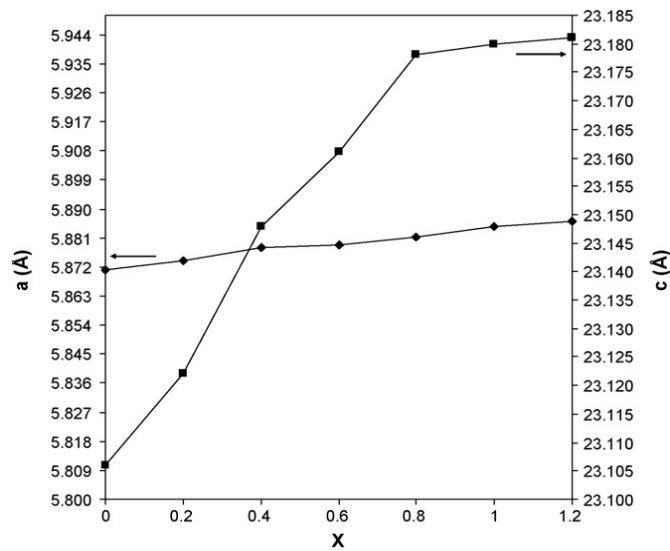


Figure 1: X-ray diffraction pattern of  $\text{Ca}(\text{CoTi})_{0.5}(\text{MnZn})_{x/2}\text{Fe}_{11-x}\text{O}_{19}$  ferrite calcinated at  $1040^\circ\text{C}$  for 96 h.



**Figure 2: Dependence of lattice constants ‘a’ and ‘c’ on substitution x in  $\text{Ca}(\text{CoTi})_{0.5}(\text{MnZn})_{x/2}\text{Fe}_{11-x}\text{O}_{19}$  ferrite.**

### 3.2. SEM

Scanning electron micrograph studies of  $\text{Ca}(\text{CoTi})_{0.5}(\text{MnZn})_{x/2}\text{Fe}_{11-x}\text{O}_{19}$  compounds reveal enhanced inter-grain connectivity through  $\text{Mn}^{4+}$  and  $\text{Zn}^{2+}$  ion substitution (Fig.3). The agglomeration of grains is attributed to increased grain size with the substitution of  $\text{Mn}^{4+}$  and  $\text{Zn}^{2+}$  ions. Table-1 shows increased cell volume, bulk density, and reduced porosity with these ion substitutions. The observed decrease in porosity is evident in SEM images, indicating closer grain proximity in various samples. The calculated density for all studied samples exceeds 84% [10].

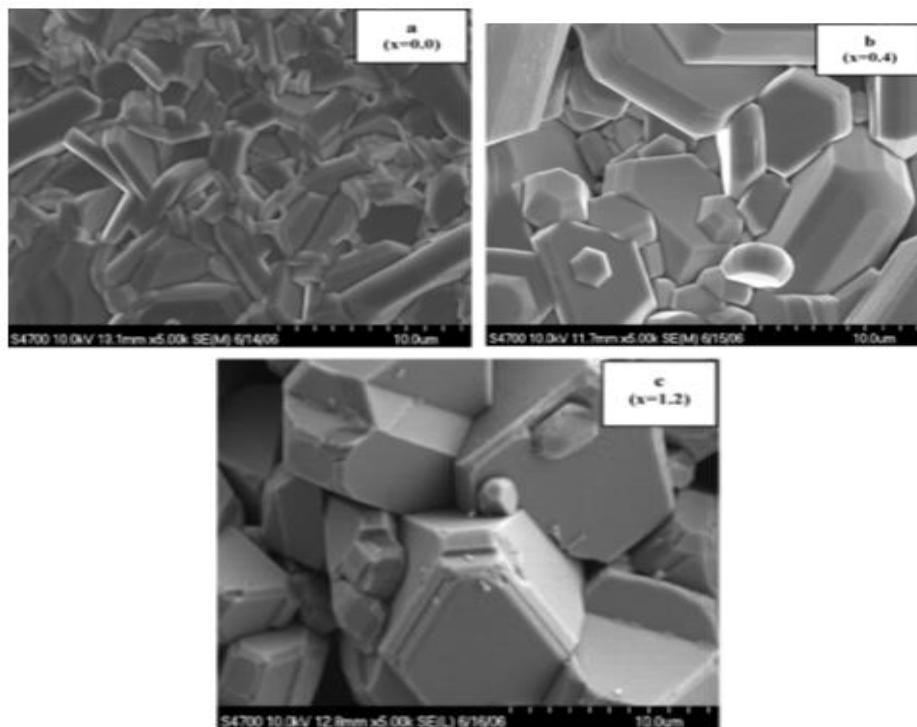


**Figure 3: SEM micrographs of ferrite samples:**  
**(a)  $\text{Ca}(\text{CoTi})_{0.5}(\text{MnZn})_{0.1}\text{Fe}_{10.8}\text{O}_{19}$ , (b)  $\text{Ca}(\text{CoTi})_{0.5}(\text{MnZn})_{0.2}\text{Fe}_{10.6}\text{O}_{19}$  and (c)  $\text{Ca}(\text{CoTi})_{0.5}(\text{MnZn})_{0.4}\text{Fe}_{10.2}\text{O}_{19}$ .**

### 3.3. SATURATION MAGNETIZATION ( $M_s$ ), COERCIVITY ( $H_c$ ) AND ANISOTROPY FIELD ( $H_a$ )

The Electronegativity of substituted ions in the  $\text{Ca}(\text{CoTi})_{0.5}(\text{MnZn})_{x/2}\text{Fe}_{11-x}\text{O}_{19}$  compounds is influenced by their occupancy in octahedral and tetrahedral sites [11]. With Electronegativity values of 1.55 for  $\text{Mn}^{4+}$  and 1.65 for  $\text{Zn}^{2+}$ ,  $\text{Mn}^{4+}$  ions prefer tetrahedral sites due to their d5 configuration, while  $\text{Zn}^{2+}$  ions favor octahedral sites owing to their d10 configuration. The specific distribution of these ions depends on the synthesis method [12]. Graphical representation of hysteresis loops (Fig. 4) shows a pronounced increase in magnetization at low applied fields, decreasing sharply at high fields. Samples with  $x = 0$  do not reach a saturation state, while all other doped samples exhibit saturation. This behavior is attributed to a significant decrease in the anisotropy field, as reflected in the coercivity ( $H_c$ ) variation graph. The saturation magnetization ( $M_s$ ) for  $x = 0$  is calculated to be 63 mu/g using the formula [13].

$$M = M_s(1 - A/H - B/H^2) + \chi_p H \quad (1)$$

$$B = \frac{H_a^2}{15} = \frac{4 K_1^2}{15 M_s^2} \quad (2)$$

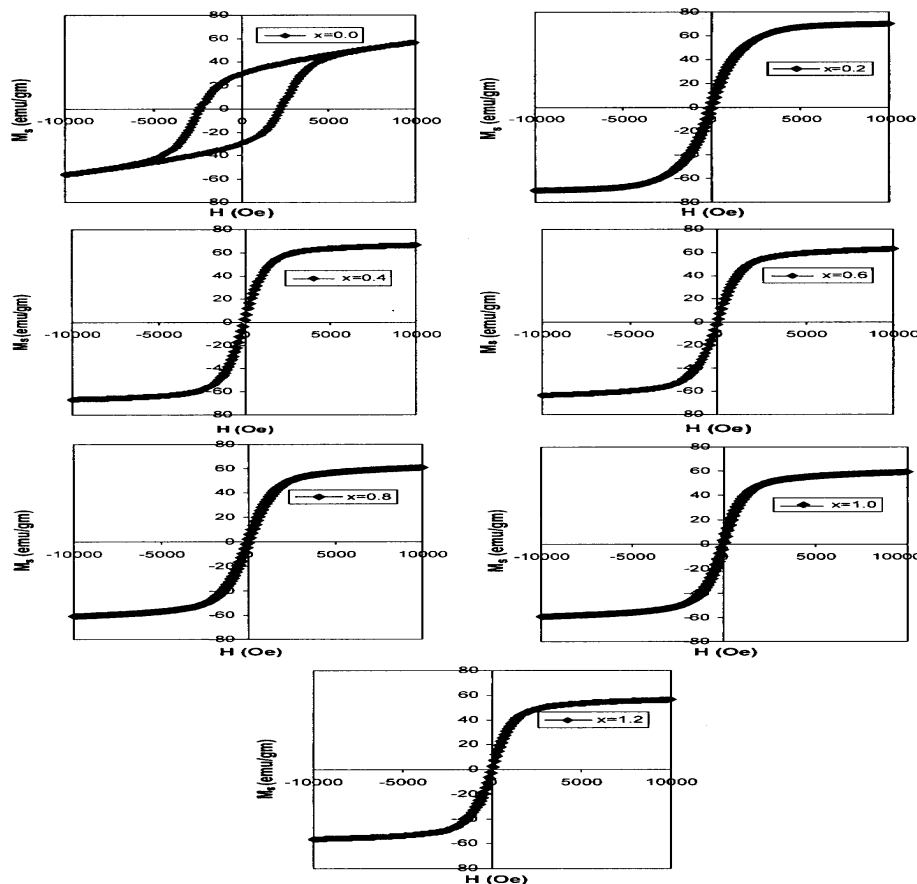


**Figure 4: Hysteresis loops of  $\text{Ca}(\text{CoTi})_{0.5}(\text{MnZn})_{x/2}\text{Fe}_{11-x}\text{O}_{19}$  ferrite ( $x = 0.0, 0.2, 0.4, 0.6, 0.8, 1.0, 1.2$ ) at room temperature.**

In M-type hexaferrites,  $\text{Fe}^{3+}$  ions occupy seven octahedral sites (12k and 2a), a trigonal bipyramidal site (2b) with spins in one direction, and two octahedral sites (4f1) and two tetrahedral sites (4f2) with spins in opposite directions. The observed high coercivity variation (Fig. 5) is attributed to strong uniaxial

magneto-crystalline anisotropy field ( $H_a$ ) and anisotropy constant ( $K_1$ ). The substitution of  $Mn^{4+}$  and  $Zn^{2+}$  ions leads to a rapid decrease in coercivity, primarily influenced by the intrinsic effect associated with the replacement of  $Fe^{3+}$  ions at 4f2 and 2b sites, which contribute to a large anisotropy field [14]. Additionally, an extrinsic effect is observed, wherein an increase in grain size due to  $Mn^{4+}$  and  $Zn^{2+}$  ion substitution (SEM Fig.3(a,b,c)) contributes to the decrease in coercivity.

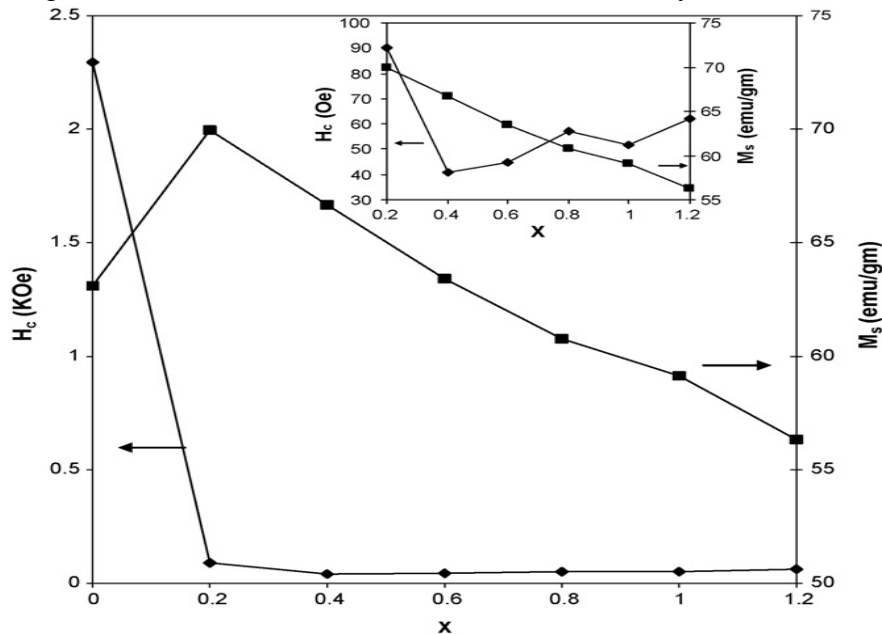


**Figure 5: Saturation magnetization ( $M_s$ ) and coercivity ( $H_c$ ) of  $Ca(CoTi)_{0.5}(MnZn)_{x/2}Fe_{11-x}O_{19}$  ferrite as a function of substitution  $x$ . Inset in the figure is for better guide to eye of coercivity variation from samples 0.2 to 1.2.**

The substitution of  $Mn^{4+}$  and  $Zn^{2+}$  ions alters the easy axis of magnetization along the c-axis of the basal plane, resulting in a significant reduction in coercivity. A 96% reduction in coercivity is observed from  $x = 0$  (2263 Oe) to  $x = 0.2$  (90 Oe), followed by a slight decrease from  $x = 0.4$  to  $x = 1.2$ , indicating a transition from hard ferrite to soft ferrite. Similar findings have been reported by Ghasemi et al. in Ba–Mn–Cu–Ti hexagonal ferrite [15]. The saturation magnetization ( $M_s$ ) increases with  $Mn^{4+}$  and  $Zn^{2+}$  ion substitution up to  $x = 0.2$ , reaching 70 emu/g compared to the undoped sample for  $x = 0$  (63 emu/g) [16]. This increase is attributed to the replacement of  $Fe^{3+}$  ions (leading to magnetization reduction) by  $Mn^{4+}$  and  $Zn^{2+}$  ions in the spin-down state, boosting saturation magnetization ( $M_s$ ). Beyond  $x = 0.2$ ,  $M_s$  decreases due to the lower magnetic moment of  $Mn^{4+}$  and  $Zn^{2+}$  ions compared to  $Fe^{3+}$  ions, although not fully offset. The relationship between  $M$  and  $1/H^2$  at 8 to 10 kOe shows a linear pattern in all samples, allowing neglect of  $A/H$  and  $\chi_p$  in Eq. (1). The slope of the straight line,  $M = M_s(1 - B/H^2)$ , allows calculation of the anisotropy parameter 'B.' Anisotropy field ( $H_a$ ) decreases rapidly from  $x = 0$  to  $x = 0.2$  due to the reduced coercivity ( $H_c$ ) [17]. The comparable curves of coercivity ( $H_c$ ) and anisotropy field ( $H_a$ ) at low substitution ( $x = 0.2$ ) suggest that anisotropic field ( $H_a$ ) predominantly influences material magnetization. In contrast, the inset in (Fig. 6) shows non-comparable coercivity ( $H_c$ ) and anisotropy field ( $H_a$ ) from  $x = 0.2$  to 1.2, indicating the influence of grain size on coercivity. The magnetic properties of Mn-Zn-substituted Ca-hexaferrite are enhanced, featuring improved  $M_s$  (70 emu/g,  $x = 0.2$ ) and lower  $H_c$  (90 Oe,  $x = 0.2$ ) [18].

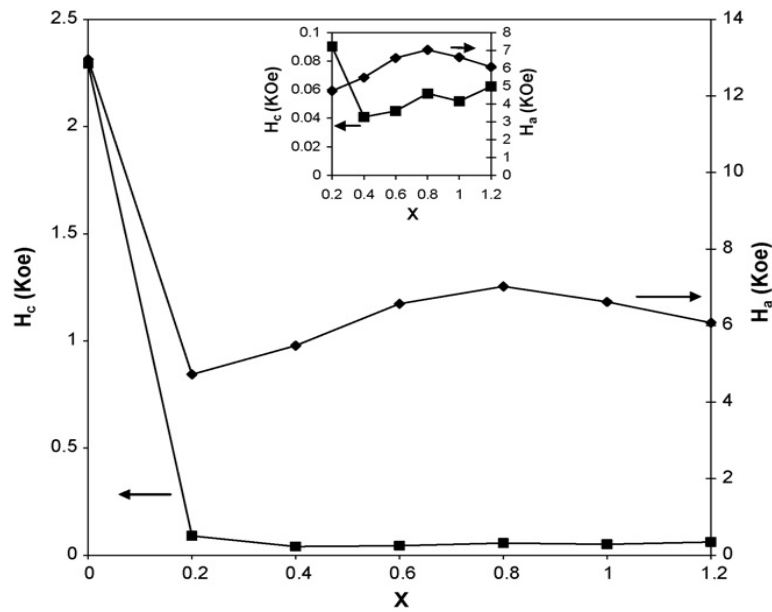


**Figure 6: Variation of  $H_a$  and  $H_c$  in  $\text{Ca}(\text{CoTi})_{0.5}(\text{MnZn})_{x/2}\text{Fe}_{11-x}\text{O}_{19}$  ferrite as a function of substitution  $x$ . Inset in the figure is for better guide to eye of  $H_a$  and  $H_c$  variation from samples 0.2 to 1.2.**

### 3.4. CURIE TEMPERATURE

Curie temperature ( $T_c$ ) exhibits a decreasing trend with the substitution of  $\text{Mn}^{4+}$  and  $\text{Zn}^{2+}$  ions, as shown in Fig. 7. This decline is attributed to the replacement of  $\text{Fe}^{3+}$  ions by  $\text{Mn}^{4+}$  and  $\text{Zn}^{2+}$  ions with lower magnetic moments, resulting in a decrease in the number of magnetic ions. The imbalanced spin alignment at lower thermal energy contributes to the observed reduction in Curie temperature ( $T_c$ ). A similar decrease in  $T_c$  due to the substitution of  $\text{Mn}^{4+}$  and  $\text{Zn}^{2+}$  ions has been reported in Ba–Cr-hexaferrites by Kim et al. [19] and in Sr–La-hexaferrites by Liu et al. [20].

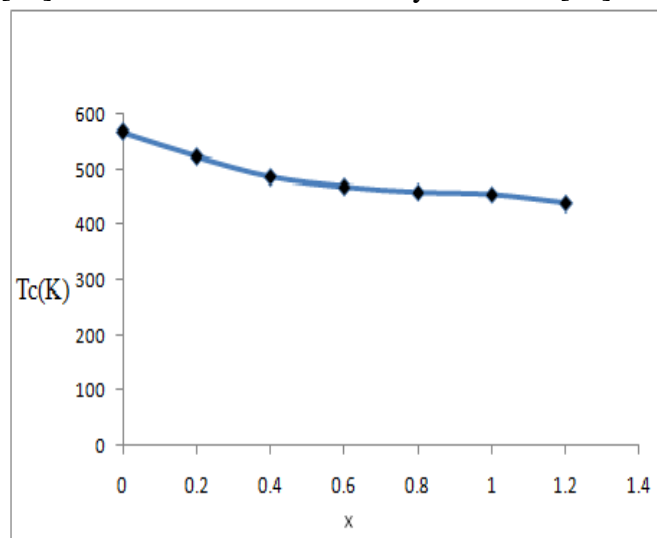


**Figure 7: Variation of Curie temperature of  $\text{Ca}(\text{CoTi})_{0.5}(\text{MnZn})_{x/2}\text{Fe}_{11-x}\text{O}_{19}$  ferrite with Mn and Zn substitution.**

**Table 1: Table shows Lattice constants ‘a’ and ‘c’, cell volume, X-ray density (D<sub>x</sub>), bulk density (D<sub>b</sub>) and porosity of Ca(CoTi)<sub>0.5</sub>(MnZn)<sub>x/2</sub>Fe<sub>11-x</sub>O<sub>19</sub> ferrite.**

Compounds	a (Å)	c (Å)	V (cm <sup>3</sup> )	D <sub>x</sub> (g/cm <sup>3</sup> )	D <sub>b</sub> (g/cm <sup>3</sup> )	Porosity (%)	T <sub>c</sub> (K)
Ca(CoTi) <sub>0.5</sub> Fe <sub>11</sub> O <sub>19</sub>	5.870	23.109	0.8831	5.1742	4.8625	0.0602	568
Ca(CoTi) <sub>0.5</sub> (MnZn) <sub>0.1</sub> Fe <sub>10.8</sub> O <sub>19</sub>	5.873	23.124	0.7983	5.1789	4.8821	0.0564	523
Ca(CoTi) <sub>0.5</sub> (MnZn) <sub>0.2</sub> Fe <sub>10.6</sub> O <sub>19</sub>	5.875	23.146	0.7612	5.1911	4.9236	0.0516	486
Ca(CoTi) <sub>0.5</sub> (MnZn) <sub>0.3</sub> Fe <sub>10.4</sub> O <sub>19</sub>	5.878	23.157	0.7329	5.1902	4.9394	0.0484	468
Ca(CoTi) <sub>0.5</sub> (MnZn) <sub>0.4</sub> Fe <sub>10.2</sub> O <sub>19</sub>	5.878	23.179	0.6323	5.1864	4.9463	0.0463	458
Ca(CoTi) <sub>0.5</sub> (MnZn) <sub>0.5</sub> Fe <sub>10</sub> O <sub>19</sub>	5.883	23.181	0.6305	5.2054	4.9786	0.0436	454
Ca(CoTi) <sub>0.5</sub> (MnZn) <sub>0.6</sub> Fe <sub>9.8</sub> O <sub>19</sub>	5.887	23.183	0.6288	5.2136	4.9962	0.0416	452

#### 4. CONCLUSIONS:

Mn-Zn-substituted Ca-hexaferrites were synthesized using a ceramic technique. The lattice constants 'a' and 'c' increased with the substitution of Mn<sup>4+</sup> and Zn<sup>2+</sup> ions, leading to a decrease in coercivity and dominant anisotropy effects. Saturation magnetization increased due to the replacement of Fe<sup>3+</sup> ions in the spin-down state compared to Mn<sup>4+</sup> and Zn<sup>2+</sup> ions. The transition from a hard phase (undoped ferrite) to a soft phase (doped ferrite) is evident, indicating a reduction in hysteresis loop area per cycle. Additionally, the Curie temperature decreased with these ion substitutions.

#### FUTURE ISSUES:

Many scientists has been done work on M-type hexaferrite. To pay attention to the real research on ferrite data obtained from last 25 years and summarized a little in this work. The main application of this developed material is in magnetic recording media, ferrofluids, sensors, microwave absorbing materials, ceramic magnets in loud speakers and rotors in small DC motors etc.

#### ACKNOWLEDGEMENT:

I expressed my sincere thanks to Dr. K. G. Rewatkar who have supported me continuously for the research activities. This type of work shows systematic research to find any problem and receiving many new results in this area. It is a lot of thanks to my colleagues for constructive support.

#### REFERENCES:

1. Y. Li, R. Liu, Z. Zhang, C. Xiong, Mater. Chem. Phys. 64 (2000) 256–259.
2. J.-H. Choy, Y.-S. Han, S.-W. Song, Mater. Lett. 19 (1994) 257–262.
3. D.E. Speliotis, IEEE Trans. Magn. 25 (1989) 4048–4050.
4. R.G. Simmons, IEEE Trans. Magn. 25 (1989) 4051–4053.
5. Q. Fang, H. Cheng, K. Huang, J. Wang, R. Li, Y. Jiao, J. Magn. Mater. 294 (2005) 281–286.
6. S.Y. An, S.W. Lee, S.W. Lee, C.S. Kim, J. Magn. Mater. 242–245 (2002) 413–415.
7. I.P. Parkin, G. Elwin, M.V. Kuznetsov, Q.A. Pankhurst, Q.T. Bui, G.D. Forster, L.F. Barquin, A.V. Komarov, Y.G. Morozov, J. Mater. Process. Technol. 110 (2001) 239–243.
8. H. Kojima, in: E.P. Wohlfarth (Ed.), Ferromagnetic Materials, vol. 3, Amsterdam, North-Holland, 1982, p. 305.

9. T.M. Meaz, C.B. Koch, *Hyperfine Interact.* 156/157 (2004) 341–346.
10. A. González-Angeles, G. Mendoza-Suares, A. Grusková, J. Slašma, J. Lipka, M. Papaňova, *Mater. Lett.* 59 (2005) 1815–1819.
11. M.V. Rane, D. Bahadur, S.D. Kulkarni, S.K. Date, *J. Magn. Magn. Mater.* 195 (1999) L256–L260.
12. Z. Šimsa, S. Lego, R. Gerber, E. Pollert, *J. Magn. Magn. Mater.* 140–144 (1995) 2103–2104.
13. R. Grossinger, *J. Magn. Magn. Mater.* 28 (1982) 137–142.
14. G. Mendoza-Suares, L.P. Rivas-Vázquez, J.C. Corral-Huacuz, A.F. Fuentes, J.I. Escalante-García, *Physica B* 339 (2003) 110–118.
15. A. Ghasemi, A. Hossienpour, A. Morisako, A. Saatchi, M. Salehi, *J. Magn. Magn. Mater.* 302 (2006) 429–435.
16. Z. Yang, C.S. Wang, X.H. Li, H.X. Zeng, *Mater. Sci. Eng. B* 90 (2002) 142–145.
17. H.-S. Cho, S.-S. Kim, *IEEE Trans. Magn.* 35 (1999) 3151–3153.
18. A. González-Angeles, G. Mendoza-Suares, A. Grusková, I. Toth, V. Jancárik, M. Papaňova, J.I. Escalante-García, *J. Magn. Magn. Mater.* 270 (2004) 77–83.
19. C.S. Kim, S.Y. An, J.H. Son, J.-G. Lee, H.N. Oak, *IEEE Trans. Magn.* 35 (1999) 3160–3162.
20. sX. Liu, W. Zhong, S. Yang, Z. Yu, B. Gu, Y. Du, *J. Magn. Magn. Mater.* 238 (2002) 207–214.